Journal of Robotics and Control (JRC)
Volume 4, Issue 2, March 2023
ISSN: 2715-5072, DOI: 10.18196/jrc.v4i2.17253

Validation of Quad Tail-sitter VTOL UAV Model in Fixed Wing Mode

Tri Kuntoro Priyambodo [1,*], Abdul Majid [2], Zaied Saad Salem Shouran [3]
[1] Department of Computer Science and Electronics, Universitas Gadjah Mada, Yogyakarta, Indonesia
[2] AMX UAV, Yogyakarta, Indonesia
[3] Bani Waleed University, Tripoli, Libya
Email: [1] mastri@ugm.ac.id, [2] abd.majid@amx-uav.com, [3] zaied.shouran@bwu.edu.ly
*Corresponding Author

This study is funded by Department of Computer Science and Electronics, Faculty of Mathematics and Natural Science, Universitas Gadjah Mada (UGM), under contract number 307/J01.1.28/PL.06.02/2022.

***Abstract*— Vertical take-off and landing (VTOL) is a type of unmanned aerial vehicle (UAV) that is growing rapidly because its ability to take off and land anywhere in tight spaces. One type of VTOL UAV, the tail-sitter, has the best efficiency. However, besides the efficiency offered, some challenges must still be overcome, including the complexity of combining the ability to hover like a helicopter and fly horizontally like a fixed-wing aircraft. This research has two contributions: in the form of how the analytical model is generated and the tools used (specifically for the small VTOL quad tail-sitter UAV) and how to utilize off-the-shelf components for UAV empirical modeling. This research focuses on increasing the speed and accuracy of the UAV VTOL control design in fixed-wing mode. The first step is to carry out analysis and simulation. The model is analytically obtained using OpenVSP in longitudinal and lateral modes. The next step is to realize this analytical model for both the aircraft and the controls. The third step is to measure the flight characteristics of the aircraft. Based on the data recorded during flights, an empirical model is made using system identification technique. The final step is to vali-date the analytical model with the empirical model. The results show that the characteristics of the analytical mode fulfill the specified requirements and are close to the empirical model. Thus, it can be concluded that the analytical model can be implemented directly, and consequently, the VTOL UAV design and development process has been shortened.**

Keywords—VTOL UAV; Quad Tail-sitter Control; Fixed-Wing Aerial Modeling; OpenVSP; System Identification; Analytical-Empirical Comparison.

I. INTRODUCTION

In recent years, the use of UAVs in the industry has been increasing rapidly, primarily for aerial mapping missions. Aerial mapping, such as precision farming, asset surveys, and monitoring, is the entrance to the industrial revolution 4.0 [1-7]. Fixed-wing UAVs are widely used in most industrial use cases. Although it has a coverage advantage, operating a fixed-wing UAV in a highly dense land-covered area, such as a forest and plantation, is challenging owing to the open space needed for take-off and landing. Operating a multi-copter is not optimal as its coverage is minimal, although it does not need open space for take-off and landing. The solution is a hybrid vertical take-off and landing (VTOL) UAV [8-26]. This type of UAV can take off, land vertically like a multi-copter, and transition to the fixed-wing mode for flight efficiency at a safe altitude [27-32]. The hybrid VTOL or usually just called VTOL UAV flight profile is illustrates in Fig. 1.

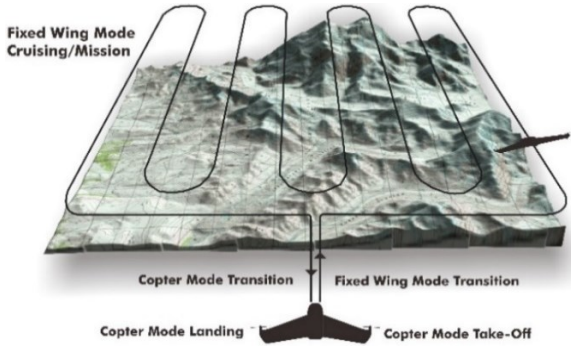

Fig. 1. VTOL UAV flight profile

Universitas Gadjah Mada collaborate with the AMX UAV company to develop a VTOL UAV, called UX-7V. The UX-7V VTOL UAV, shown in Fig. 2, was specifically designed for aerial mapping and survey missions. It is a quad tail-sitter with flying wing configuration [33]. The UX-7V VTOL UAV control system is being developed using a model-based design approach [34][35]. Building a mathematical flight model is mandatory to facilitate aircraft attitude and motion studies [36-40]. Each flight model has its characteristics called model parameters [41]. A manned aircraft usually uses a wind tunnel test to obtain the model parameters [42]. This method has the best accuracy result, but limited wind tunnel test facilities in Indonesia and the associated high costs are the challenges to implement on small UAVs.

Fig. 2. UX-7V VTOL UAV

The UX-7V UAV currently uses elevon to control the movement in fixed-wing mode [43]. The quad tail-sitter configuration [44] adopted in this UAV enables to use of differential thrust control [45]. So, in this study, the flight model will be used to develop a differential thrust control method in the subsequent research. This research focuses on a fixed-wing mode flight model using analytical modeling based on this requirement. Since the UX-7V is a successor of the UX-6 UAV [46], we used the same analytical modeling procedure as the previous study, but the tools used were different because the UX-6 UAV analytical model result is not good enough. Many tools can be used to build analytical models, such as OpenVSP [47], Datcom+Pro [48], Flow5 [49], and Tornado VLM [50]. OpenVSP software was used to develop and process the analytical model in this study. OpenVSP is widely used for preliminary design reviews on aircraft development. OpenVSP calculates aircraft aerodynamic derivatives using the vortex lattice and panel methods [50]. The aerodynamic derivatives are then used to derive model parameters. In the last step, the analytical model obtained from OpenVSP is validated with an empirical model built using system identification or reverse modeling [51-56]. This research has two contributions. The first is in the form of how the analytical model is generated and the tools used, in particular for the small VTOL quad tail-sitter UAV. The second is how to utilize off-the-shelf components for UAV empirical modeling.

II. Materials and Methods

This research follows what we performed in a previous study [43]. There are three differences, the first is the aircraft type, change from UX-6 fixed-wing UAV to UX-7V VTOL UAV. The second is the type of electronic device used. We use a commercial flight controller with custom code to control the aircraft and flight data logging. The last, the software used, which previously used Datacom+ Pro, was replaced with OpenVSP. The general research flow shown in Fig. 3.

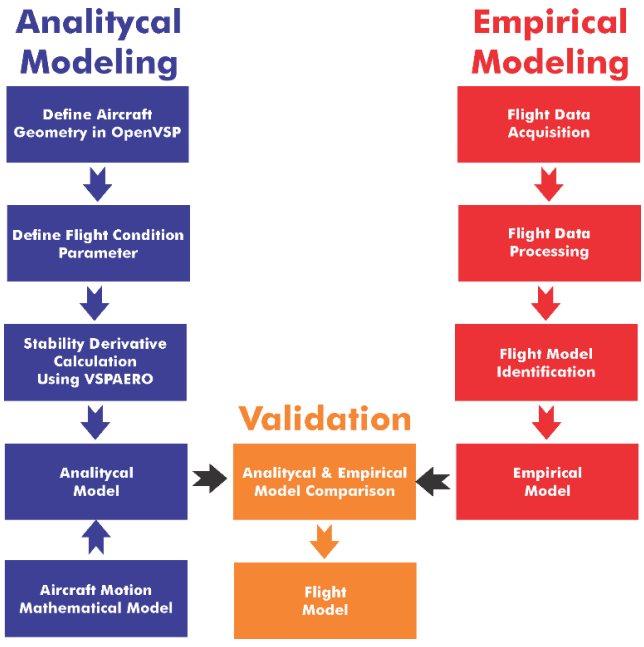

Fig. 3. The research flow of UX-7V VTOL UAV modeling in fixed wing mode

A. Quad Tail-sitter

Tail-sitter or tilt body is one of hybrid VTOL type [56], that had two orientations:

- Vertical orientation for take-off and landing is similar to a copter.
- Horizontal orientation for a forward flight is similar to a fixed-wing.

Tail-sitters generally have two (dual) or four (quad) motors configuration. All tail-sitter motors keep running, both vertically and horizontally. In this research, the UX-7V UAV has a quad tail-sitter configuration. Quad tail-sitters typically use a flying-wing configuration. The airframe consists of a blended fuselage and wings. In the fixed-wing mode, elevons were used to control the flight. Elevons are two parts mixed on one control surface: elevators and ailerons. Elevators for up-down movements and ailerons for right-left turn movements. Fig. 4 shows the design of the quad tail-sitter UAV.

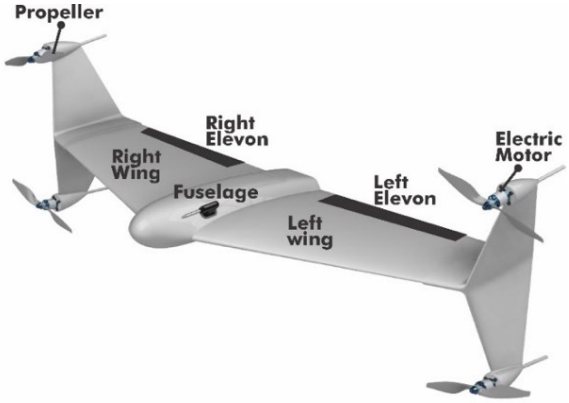

Fig. 4. Design of quad tail-sitter UAV

B. The Hardware

The three modules used in this research are a UX-7V aircraft, a remote controller (RC), and telemetry. UAV operator controls the UX-7V flight through an RC transmitter, and the ground control operator monitors the aircraft on a laptop via telemetry. Fig. 5 shows the connections and electronic devices.

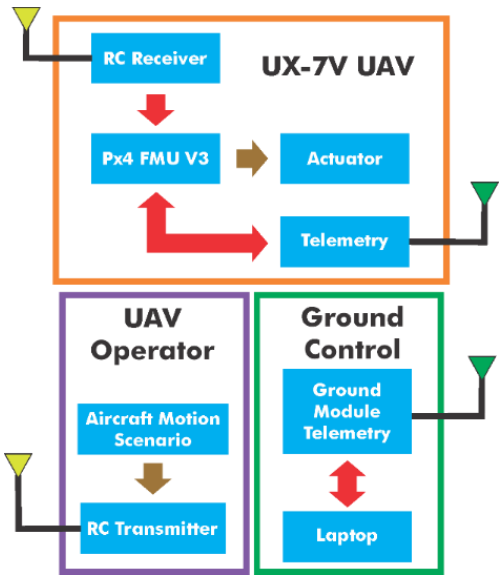

Fig. 5. The hardware diagrams

The UX-7V UAV uses PX4 based flight controller with a custom code. There are two commands to control UX-7V. First, control by a remote controller (RC), and second, by ground control/telemetry. Three modes are available: manual/stabilized, position-assisted, and autonomous. PX4 has the capability to log data, which is very useful because an operator input for actuators and output data (aircraft attitude) can be recorded at a specific rate. The PX4 data log is set to run at 5 Hz, whereas the maximum aircraft movement is at 2 Hz [57]. Fig. 6 shows aircraft electronic device block diagram, and Table I lists the aircraft hardware and specification details.

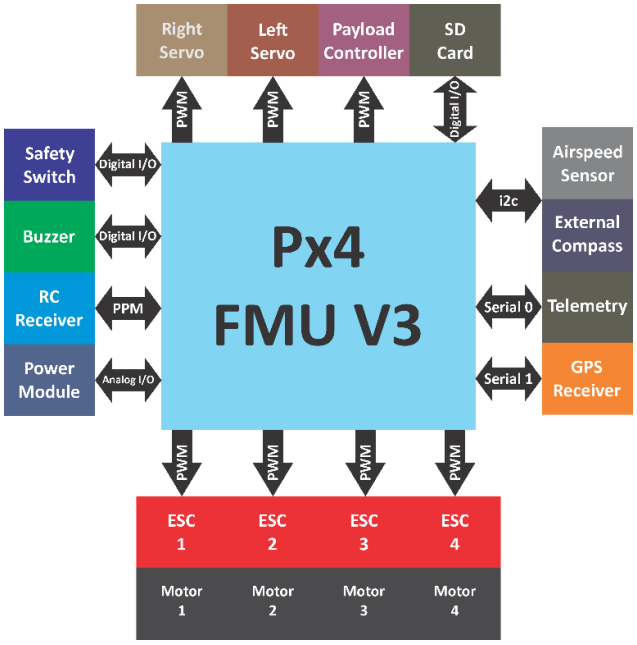

Fig. 6. UX-7V aircraft electronics devices block diagram

C. Analytical Modeling

In fixed-wing mode flight, many forces act, i.e., velocities, moments, and orientations. All could be summarized and visualized in Fig. 7.

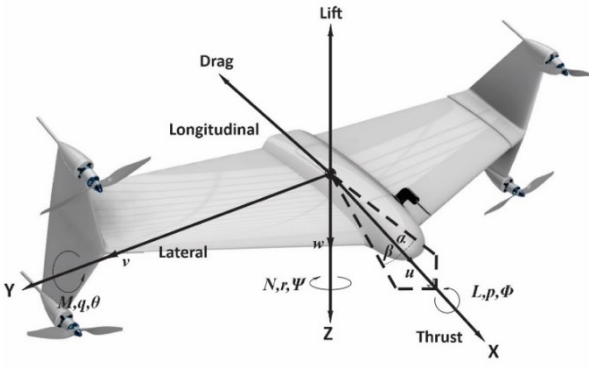

Fig. 7. Aircraft forces, velocities, moments, and orientations definitions

In flight, the aircraft is not always horizontally straight when flying ahead (on the X-axis, see Fig. 7) but has an angle of attack commonly written as α (alpha). The aircraft's angle of attack is the deflection angle of the aircraft on the x-axis caused by the wing geometry of the aircraft. Similar to the angle of attack, there is also a sideslip angle (Fig. 6), typically written as β (beta). The difference is that the sideslip angle is the deflection on the y-axis owing to the air/wind from the side that concerns the aircraft's vertical stabilizer. Equations (1) and (2) are for finding α and β.

$$\alpha = \tan^{-1}\frac{w}{u} \quad (1)$$

$$\beta = \tan^{-1}\left(\frac{v}{\sqrt{u^2 + w^2}}\right) \quad (2)$$

TABLE I. AIRCRAFT HARDWARE AND SPECIFICATION

Hardware		Specification
Aircraft	UX-7V UAV	▪ Flying wing quad tail-sitter configuration ▪ Composite material ▪ 1.4m Wingspan ▪ 3.5Kg weight
Actuator	*Electric motor*	▪ Brushless 980KV ▪ 10inch propeller ▪ 1900gr Thrust
	Servo	▪ 5-6 V ▪ Torque 2.5 Kg ▪ 13gr Weight
Flight Controller/ Recorder	PX4 FMU V3	▪ 168MHz STM32 Microcontroller ▪ L3GD20 Gyroscope ▪ LSM303D Accelerometer/ Magnetometer ▪ MPU6000 Accelerometer/ Magnetometer ▪ MS5611 Barometer ▪ UBlox M8N GPS ▪ Micro SD card storage
Radio Controller	Taranis QX7	▪ PPM receiver output ▪ 2.4GHz frequency ▪ 16 Channel transmitter ▪ 6 Channel receiver
Telemetry	RFD900X	▪ Serial TTL ▪ 915MHz frequency
Power Source	LiPo Battery	▪ 4 cell 14.8V 10AH

The Euler angle was used for the aircraft orientation as shown in Fig. 8, which has the following reference:

a. The $z-axis$ leads downward (in the same direction as the gravity vector). The angle rotation on this axis is called the yaw (ψ).

b. The $x-axis$ leads forward. The angle rotation on this axis is called the roll (φ).

c. The $y-axis$ leads rightward. The angle rotation on this axis is called the pitch (θ).

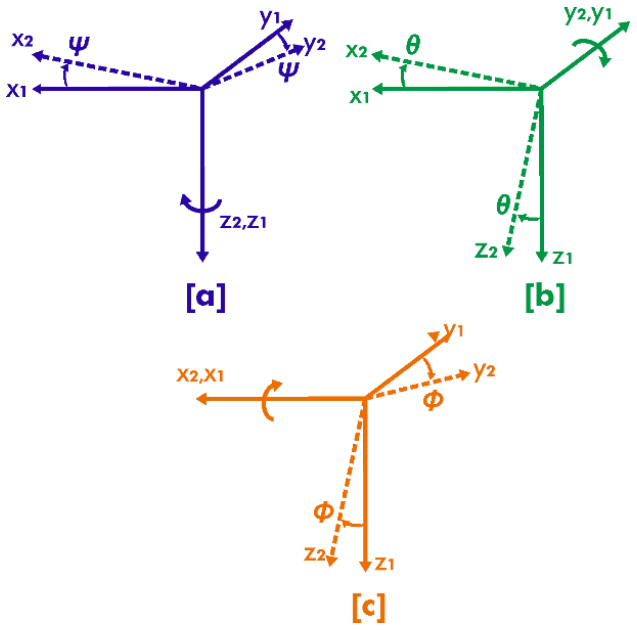

Fig. 8. Euler angle Φ, θ, and ψ to determine the aircraft's orientation. [a] Yaw rotation on the z-axis [b] pitch rotation on the y-axis. [c] roll rotation on the x-axis

One of the parameters used in aircraft motion modeling is the angular velocity along the $x-$, $y-$, and $z-axes$. The angular velocity is called the variables p, q, and r. To find, Equation (3) is used.

$$\begin{bmatrix} p \\ q \\ r \end{bmatrix} = \begin{bmatrix} 1 & 0 & -sin\theta \\ 0 & cos\phi & cos\theta sin\phi \\ 0 & -sin\phi & cos\theta cos\phi \end{bmatrix} \begin{bmatrix} \phi' \\ \theta' \\ \psi' \end{bmatrix} \quad (3)$$

where:

$$\phi', \theta', \psi' = \frac{d\phi}{dt}, \frac{d\theta}{dt}, \frac{d\psi}{dt}$$

In addition to the angular velocity, translation velocities are required for the $x-$, $y-$, and $z-axes$. The translational velocities of each axis are denoted as variables u, v, and w. The variables u, v, and w are determined by data changes in longitude, latitude, and altitude. It is then combined with the orientation of the Euler angle, thus producing u', v', and w' derived in Equation (4).

$$\begin{bmatrix} \frac{dx}{dt} \\ \frac{dy}{dt} \\ \frac{dz}{dt} \end{bmatrix} = \begin{bmatrix} C\theta C\psi & S\phi S\theta C\psi - C\phi S\psi & C\phi S\theta C\psi + S\phi S\psi \\ C\theta S\psi & S\phi S\theta S\psi + C\phi C\psi & C\phi S\theta S\psi - S\phi C\psi \\ -S\theta & S\phi C\theta & C\phi C\theta \end{bmatrix} \begin{bmatrix} u \\ v \\ w \end{bmatrix} \quad (4)$$

where,

$$S\phi, S\theta, S\psi = \sin\phi, \sin\theta, \sin\psi$$

$$C\phi, C\theta, C\psi = \cos\phi, \cos\theta, cos\psi$$

The flight dynamics that work on a fixed wing can be divided into longitudinal and lateral modes [58-62]. The longitudinal modes include translational motion on the x- and z-axes and rotational motion around the y-axis. The rotary motion around the y-axis changed the pitch angle. The motion in the longitudinal mode plays a role in the upward and downward movement of the aircraft. In the dynamics of aircraft flying, the longitudinal mode is influenced by the thrust and elevator. The longitudinal mode is determined using Equations (5), (6), (7), and (8).

- Forces

$$u' + qw - rv = X/m - g\, sin\theta \quad (5)$$

$$w' + pv - qu = Z/m + g\, cos\theta\, cos\phi \quad (6)$$

- Moment

$$M = I_y q' + rp(I_x - I_y) + I_{xz}(p^2 - r^2) \quad (7)$$

- Pitch orientation

$$\theta' = q\, cos\phi - r\, sin\phi \quad (8)$$

The lateral mode includes translational motion on the $y-axis$ and rotational motion along the $x-$ and $z-axes$. The lateral mode is affected by the aileron. The lateral or directional mode is used for aircraft's turning movement. The lateral mode is determined using Equations (9), (10), (11), and (12).

- Forces

$$v' + ru - pw = \frac{Y}{m} + g\, cos\theta_0\, sin\phi \quad (9)$$

- Moments

$$L = I_x p' - I_{xz} r' + qr(I_z - I_y) - I_{xz} pq \quad (10)$$

$$N = -I_{xz} p' + I_z r' + pq(I_y - I_x) + I_{xz} qr \quad (11)$$

- Roll orientation

$$\phi' = p + (q\, sin\phi - r\, cos\phi)\, tan\theta \quad (12)$$

Both longitudinal and lateral modes are necessary for all equations that work to elaborate and add flight assumptions (linear model and ignore flight disturbances such as wind, thermal, and weather). Then, we obtain the general equations of the longitudinal mode flight model in the form of a state-space model structure [63], [64] in Equation (13).

$$\begin{bmatrix} \Delta\dot{u} \\ \Delta\dot{\alpha} \\ \Delta\dot{q} \\ \Delta\dot{\theta} \end{bmatrix} = \begin{bmatrix} X_u & X_w & X_q + w_0 & -gcos\theta_0 \\ \frac{Z_u}{u_0} & \frac{Z_w}{u_0} & Z_q - w_0 & \frac{-gsin\theta_0}{u_0} \\ M_u & M_w & M_q & 0 \\ 0 & 0 & \cos\phi_0 & 0 \end{bmatrix} \begin{bmatrix} \Delta u \\ \Delta\alpha \\ \Delta q \\ \Delta\theta \end{bmatrix} + \begin{bmatrix} X_{\delta_e} & X_{\delta_T} \\ Z_{\delta_e} & 0 \\ M_{\delta_e} & 0 \\ 0 & 0 \end{bmatrix} \begin{bmatrix} \Delta\delta_e \\ \Delta\delta_T \end{bmatrix} \quad (13)$$

Furthermore, the lateral mode is the same as the longitudinal mode. Equation (14) represents the general equation for the lateral mode flight model.

$$\begin{bmatrix} \Delta\dot{\beta} \\ \Delta\dot{p} \\ \Delta\dot{r} \\ \Delta\dot{\phi} \end{bmatrix} = \begin{bmatrix} \frac{Y_u}{u_0} & \frac{Y_p + w_0}{u_0} & \frac{-(u_0 - Y_r)}{u_0} & \frac{gcos\theta_0}{u_0} \\ L_v & L_p & L_r & 0 \\ N_v & N_p & N_r & 0 \\ 0 & 1 & \tan\theta_0 & 0 \end{bmatrix} \begin{bmatrix} \Delta\beta \\ \Delta p \\ \Delta r \\ \Delta\phi \end{bmatrix} + \begin{bmatrix} 0 \\ L_{\delta_a} \\ N_{\delta_a} \\ 0 \end{bmatrix} [\Delta\delta_a] \quad (14)$$

The general linear equations of the longitudinal and lateral modes are obtained, and each variable is filled with values corresponding to the characteristics of the aircraft modeled using the OpenVSP software calculation.

D. Flight Data Acquisition

Flight data acquisition records an input signal given to the actuator, and the output data includes the aircraft's attitude, position, and speed. The input must be prepared. Several input scenarios are commonly used for identification systems, such as 3-2-1-1 and doublet input [65]. We use doublet input, a variety of inputs where a high position of the actuator was given during time t and then changed to a low value of actuator during time t. The signal is sent to the aircraft actuator through an RC transmitter. Doublet inputs are used by researchers and manufacturers to identify aircraft [66-76]. Fig. 9 shows the shape of the input doublet signal.

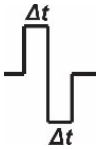

Fig. 9. Doublet input

Because this research divides the modeling into longitudinal and lateral modes, each mode is given a different doublet input, elevator in the longitudinal mode, and aileron in the lateral mode. The aircraft was conditioned in level flight condition during flight data acquisition before being given doublet input. Fig. 10 shows the flight data acquisition procedure.

The data log feature in the PX4 flight controller was customizable. The data groups selected for storage are as follows:

- actuator_controls_1
- airspeed
- vehicle_attitude
- vehicle_gps_position

The recorded flight data are then processed and converted into a variable used for system identification. Because the recorded vehicle attitude is in aircraft copter mode, while system identification uses fixed-wing mode attitude, quaternion rotation is required. It changes y-axis orientation by 90 degrees. Fig. 11 shows quaternion rotation.

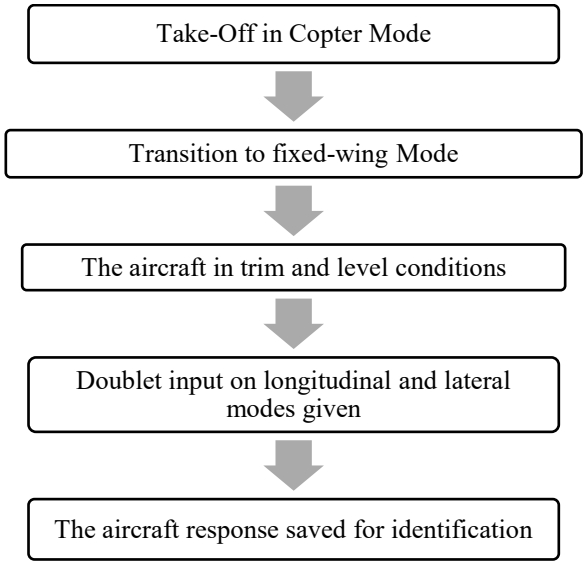

Fig. 10. UX-7V UAV flight data acquisition procedures

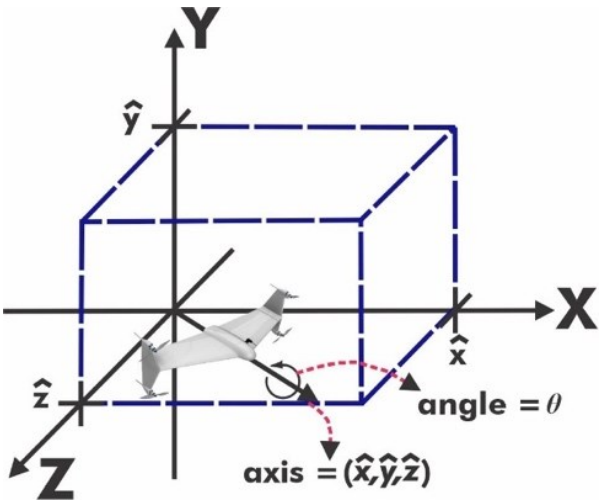

Fig. 11. Rotation in quaternion

If we know the axis and angle components $(\theta, \hat{x}, \hat{y}, \hat{z})$, we can convert to a quaternion rotation p using Equation (15) [77].

$$p = [p_0, p_1, p_2, p_3] \tag{15}$$

where:

$$p_0 = \cos\left(\frac{\theta}{2}\right)$$

$$p_1 = \hat{x}\sin\left(\frac{\theta}{2}\right)$$

$$p_2 = \hat{y}\sin\left(\frac{\theta}{2}\right)$$

$$p_3 = \hat{z}\sin\left(\frac{\theta}{2}\right)$$

Thus, the attitude vehicle data, which rotates the aircraft by 90 degrees on the $\boldsymbol{y}$-axis is p:

$$p = [0.7071, 0, 0.7071, 0]$$

If the copter mode attitude is q, we can obtain the fixed-wing mode attitude t by multiplying by Equation (16).

$$t = qp \tag{16}$$

where:

$$(t_0, t_1, t_2, t_3) = (q_0, q_1, q_2, q_3) \times (q_0, q_1, q_2, q_3)$$

$$t_0 = r_0 s_0 - r_1 s_1 - r_2 s_2 - r_3 s_3$$

$$t_1 = r_0 s_1 - r_1 s_0 - r_2 s_3 - r_3 s_2$$

$$t_2 = r_0 s_2 - r_1 s_3 - r_2 s_0 - r_3 s_1$$

$$t_3 = r_0 s_3 - r_1 s_2 - r_2 s_1 - r_3 s_0$$

After the attitude data are appropriate, the next step is to convert the quaternion angle into an Euler angle [42] using Equation (17).

$$\begin{bmatrix}\phi \\ \theta \\ \psi\end{bmatrix} = \begin{bmatrix}atan2(2(q_0 q_1 + q_2 q_3), 1 - 2(q_1^2 + q_2^2)) \\ asin(2(q_0 q_2 + q_3 q_1), \\ atan2(2(q_0 q_3 + q_1 q_2), 1 - 2(q_2^2 + q_3^2))\end{bmatrix} \tag{17}$$

All flight data process is shown in Fig. 12.

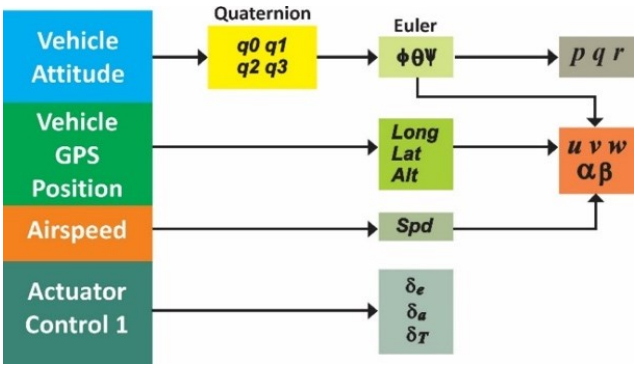

Fig. 12. The flight data processing diagram

E. Empirical Modeling

An empirical model was built to validate the analytical model. The empirical model is based on flight data obtained through flight data acquisition, which is processed using a system identification technique [78]. Conceptually, system identification is a dynamic system shown in Fig. 13, modeling from the data generated in the experiment.

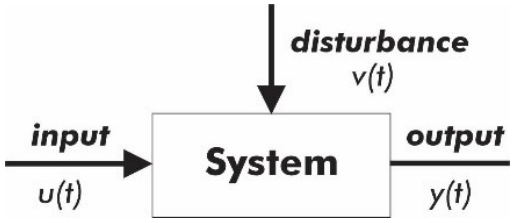

Fig. 13. Dynamic system with input u(t), output y(t), and disturbance v(t), where t represents time

In system identification, there are three parameters:

- Input and output data.
- Model structure.
- Model criteria.

This study uses a state-space model structure to build the empirical model, which has the same structure as the analytical model. The typical state-space model structure is different from the analytical model known as black-box system identification [79]. Fig. 14 shows MATLAB software used for system identification, precisely one of the sub-tools, the system identification toolbox.

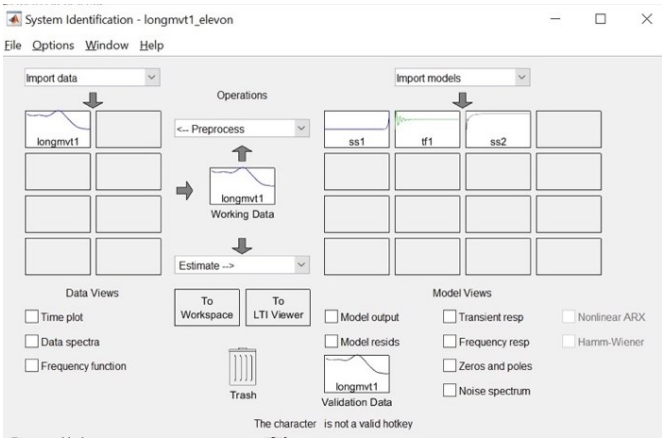

Fig. 14. System identification toolbox in MATLAB

III. Results

A. Flight Data Acquisition

The flight data acquisition shown in Fig. 15 was performed at 7 AM to obtain clear and relatively no-wind conditions [80][81]. We performed several flights; one determined the primary data and the other for backup. Fig. 16 shows the UX-7V main data flight path.

Fig. 15. UX-7V during flight data acquisition

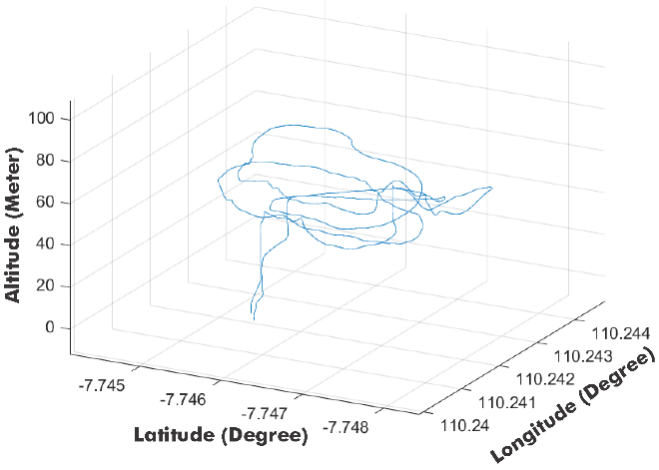

Fig. 16. UX-7V data acquisition flight path

B. Empirical Model

The aircraft trim conditions [82] can be determined based on UX-7V UAV flight data. The trim condition is an aircraft condition when $u \neq 0$, $w = 0$, $q = 0$, and $\theta \neq 0$. The UX-7V UAV trim conditions are shown in Table II.

TABLE II. UX-7V VTOL UAV Trim Condition

Parameter	Value (radian)
Pitch angle (θ)	0.1221
Roll angle (ϕ)	0.061
Elevator deflection (δ_e)	0.0785
Aileron deflection (δ_a)	0.034

After the flight data were processed using the system identification toolbox in MATLAB, an empirical model that represents UX-7V VTOL UAV was built, Equation (18) for longitudinal mode and Equation (19) for lateral mode.

$$\begin{bmatrix}\Delta\dot{u}\\ \Delta\dot{\alpha}\\ \Delta\dot{q}\\ \Delta\dot{\theta}\end{bmatrix}=\begin{bmatrix}-2.06 & -0.8598 & 0.6545 & -0.4687\\ 0.8527 & -0.3531 & 0.1122 & -0.3356\\ -5.206 & -1.829 & 0..9468 & -0.6839\\ -0.5721 & 0.8309 & -0.2646 & 0.5951\end{bmatrix}\begin{bmatrix}\Delta u\\ \Delta\alpha\\ \Delta q\\ \Delta\theta\end{bmatrix}+\begin{bmatrix}0.1546 & -2.165\\ -3.791 & 0.111\\ 6.873 & -2.359\\ 10.11 & 3.242\end{bmatrix}\begin{bmatrix}\Delta\delta_e\\ \Delta\delta_T\end{bmatrix} \quad (18)$$

$$\begin{bmatrix}\Delta\dot{\beta}\\ \Delta\dot{p}\\ \Delta\dot{r}\\ \Delta\dot{\phi}\end{bmatrix}=\begin{bmatrix}-4.653 & -11.41 & -0.3716 & 0.9347\\ 1.271 & 1.399 & -0.0059 & -0.3162\\ -8.28 & -4.475 & 0.3711 & 3.118\\ 0.306 & -1.355 & -0.1383 & -0.2519\end{bmatrix}\begin{bmatrix}\Delta\beta\\ \Delta p\\ \Delta r\\ \Delta\phi\end{bmatrix}+\begin{bmatrix}-0.7712\\ 0.2382\\ 2.078\\ 1.149\end{bmatrix}[\Delta\delta_a] \quad (19)$$

C. *Analytical Model*

The analytical model used OpenVSP to obtain static and dynamic aerodynamic coefficients. This research use a panel method for the calculation [47]. The panel method models many elementary quadrilateral panels lying on an actual aircraft surface [83]. The OpenVSP calculation requires aircraft geometry data and aircraft flight conditions. The flight condition was equated with the UX-7V UAV level flight condition, obtained from flight data acquisition. The UX-7V UAV level flight condition was predicted at 7 degrees AoA, 17m/s velocity, and a 50-meter altitude. The UX-7V UAV geometry data and flight conditions input into OpenVSP generated the aircraft's calculated aerodynamic coefficients. Fig. 17 depicts the UX-7V UAV 3D.

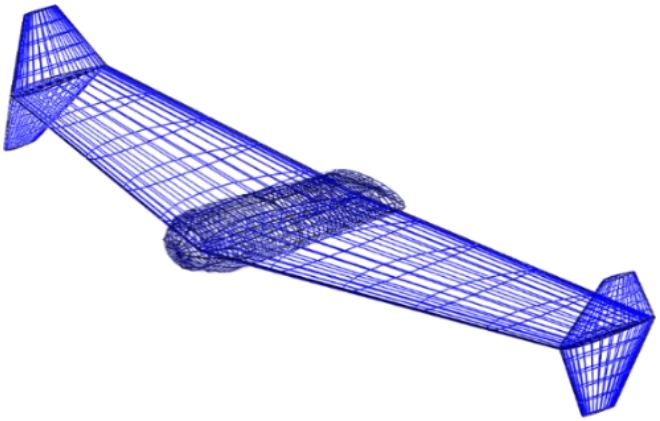

Fig. 17. UX-7V 3D model generated by OpenVSP

The static and dynamic aerodynamic coefficients generated by OpenVSP were used to calculate the stability derivative. The resulting stability derivative is organized into Equations (13) and (14). The analytical model of the UX-7V UAV is shown in Equation (20) for longitudinal mode and in Equation (21) for lateral mode.

$$\begin{bmatrix}\Delta\dot{u}\\ \Delta\dot{\alpha}\\ \Delta\dot{q}\\ \Delta\dot{\theta}\end{bmatrix}=\begin{bmatrix}-1.794 & 0.3906 & -0.1138 & 9.7874\\ 0.1856 & -6.7841 & 14.9501 & -0.6656\\ 62.5064 & -488.2926 & -329.3868 & 0\\ 0 & 0 & 1.0 & 0\end{bmatrix}\begin{bmatrix}\Delta u\\ \Delta\alpha\\ \Delta q\\ \Delta\theta\end{bmatrix}+\begin{bmatrix}0.2842 & 1.2685\\ -5.9211 & 0\\ -2.4 & 0\\ 0 & 0\end{bmatrix}\begin{bmatrix}\Delta\delta_e\\ \Delta\delta_T\end{bmatrix} \quad (20)$$

$$\begin{bmatrix}\Delta\dot{\beta}\\ \Delta\dot{p}\\ \Delta\dot{r}\\ \Delta\dot{\phi}\end{bmatrix}=\begin{bmatrix}-3.003 & -4.5 & -1.46 & -9.5040\\ 0.8486 & -66.514 & -2.6385 & 0\\ -0.0759 & -0.1138 & -0.15084 & 0\\ 0 & 1 & 0.255 & 0\end{bmatrix}\begin{bmatrix}\Delta\beta\\ \Delta p\\ \Delta r\\ \Delta\phi\end{bmatrix}+\begin{bmatrix}0\\ -68.4010\\ -0.4503\\ 0\end{bmatrix}[\Delta\delta_a] \quad (21)$$

IV. DISCUSSION

A. *Empirical Model*

The empirical model results were validated using simulation. The empirical model was compared with actual flight data in a simulation. The empirical model input was the aircraft input data. Then, the model's output was compared with the aircraft output data. The empirical model validation results showed that the model's accuracy was quite good: 90.97 percent on average for the longitudinal mode and 91.02 percent for the lateral mode. Fig. 18 and Fig. 19 shows the empirical model validation results for the longitudinal and lateral mode.

Generally, these empirical model results are better than previous research [46]. Previous research results showed an average accuracy of 73.95% for the longitudinal mode and 75.83% for the lateral mode. The UX-7V VTOL UAV already uses a flight controller, so the operator can use a position-assisted flight mode. This differs from previous research, which the operator manually controlled the aircraft movement. The UX-7V VTOL UAV operator can easily control the aircraft in a position-assisted flight mode [84][85]. The altitude and position are locked in this mode by the computed trajectory of the flight controller [86][87][88]. Therefore, the input to the empirical model of this research is not the remote-control input from the operator but the command given to the actuator from the flight controller. The accuracy of the empirical model increased drastically through this approach by approximately 20 percent.

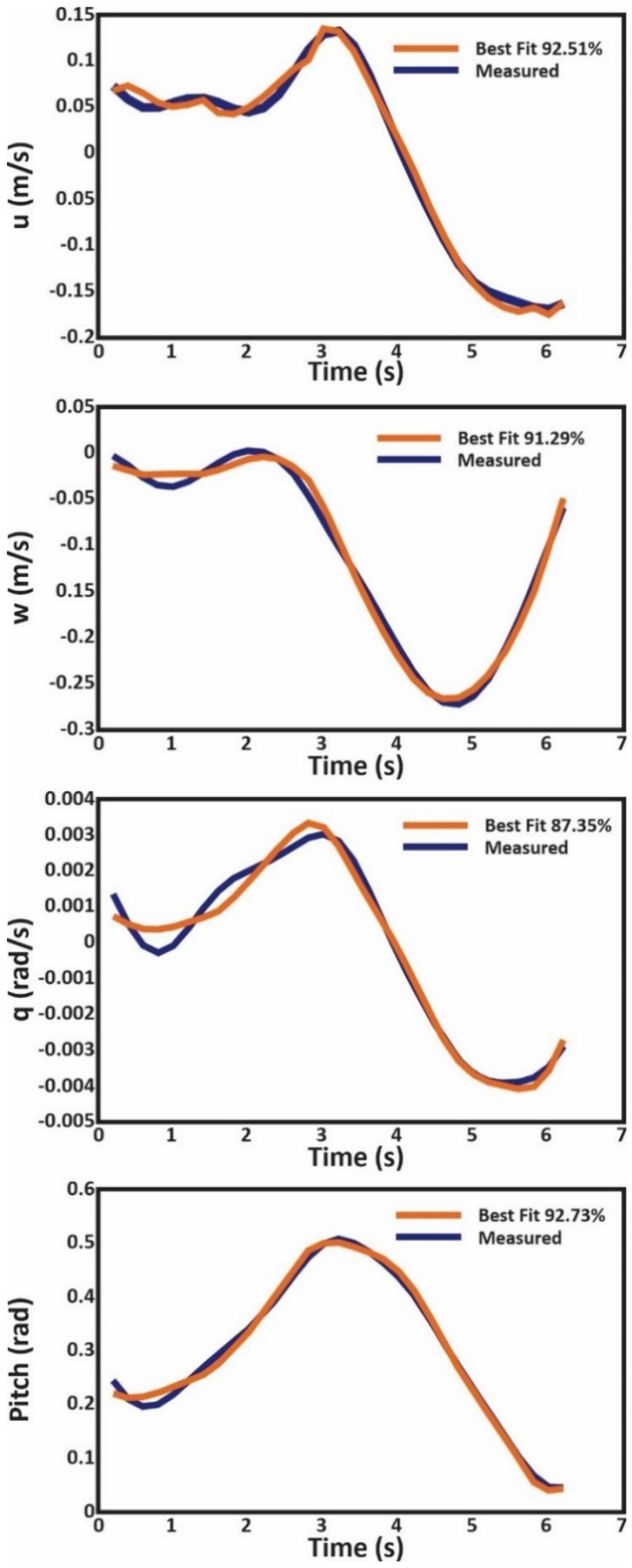

Fig. 18. Longitudinal mode Empirical model validation results

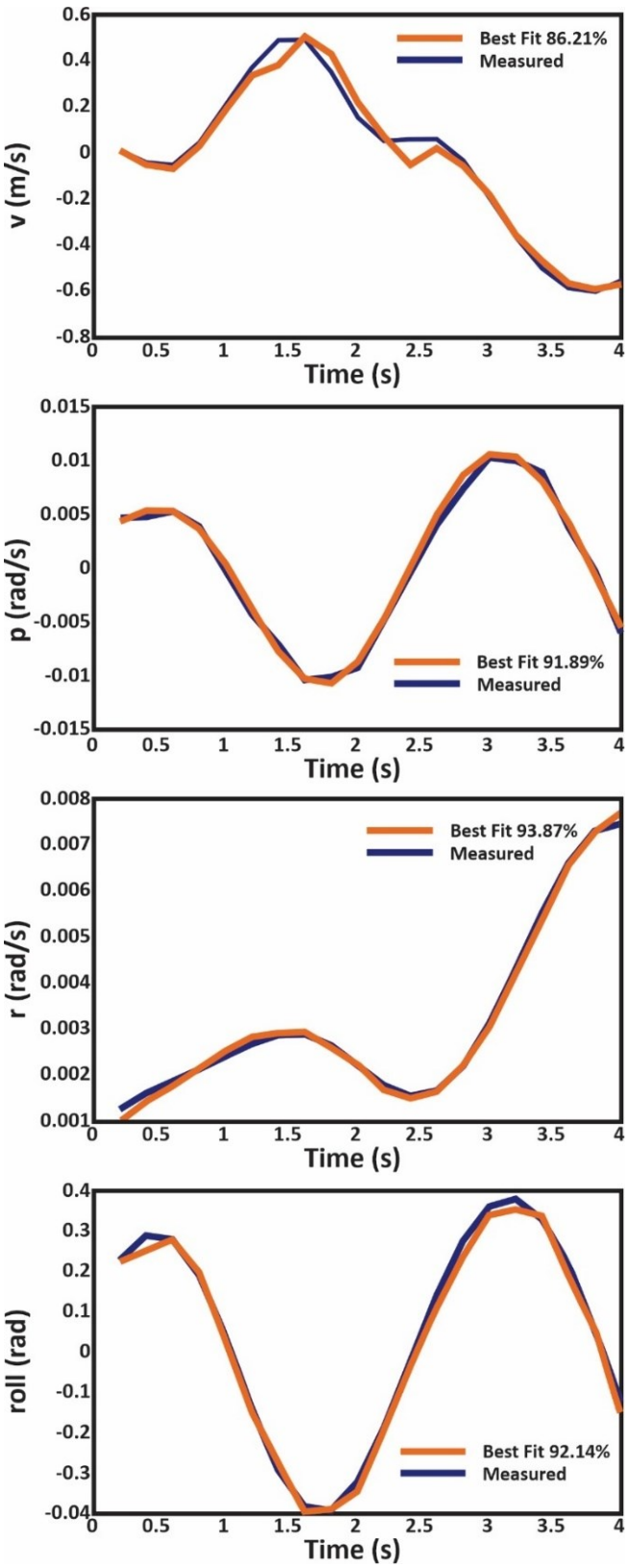

Fig. 19. Lateral mode empirical model validation results

B. Analytical Model Validation

The analytical models were built, validated using the empirical model. The process was performed by given the doublet input shown in Fig. 20 to both models. The input given is in the form of a control surface deflection of 0.6 (34.3775 degree) radians for 1 second and -0.6 radians (-34.3775 degree) for 1 second.

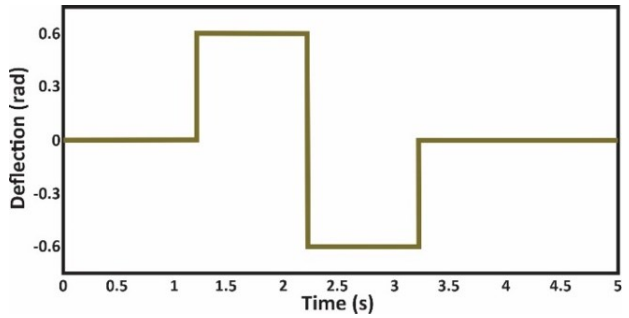

Fig. 20. Doublet input for elevator (longitudinal mode) and aileron (lateral mode)

In the longitudinal mode validation, the input doublet on the elevator is connected to the empirical and analytical models. Since the variation input is only elevator control surface, the input for throttle assumes as zero. Both models have a state-space model structure. The four output parameters of the model, namely u forward velocity, α angle-of-attack, q angular velocity, and θ angle, are then displayed in graphical form and stored for further analysis. For analytical model validation needs, MATLAB/Simulink software is used with a block diagram as shown in Fig. 21.

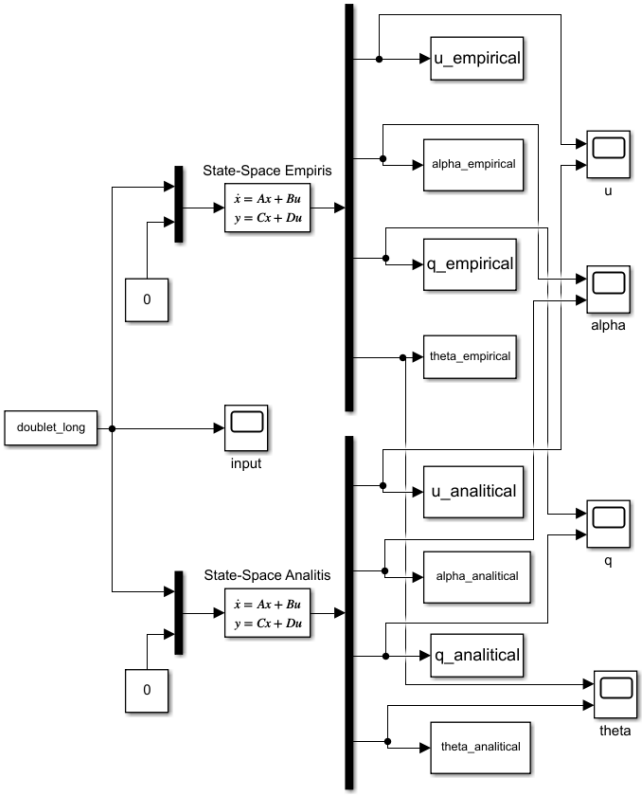

Fig. 21. Longitudinal mode validation Simulink block diagram

Fig. 22 shows the validation results of the UX-7V UAV between the analytical and empirical models in longitudinal mode. The longitudinal mode validation results showed that the longitudinal mode (u) parameter was identical. For the other three parameters (alpha (α), q, and theta (θ)), even though they have the same direction, the values are quite different. The main factor is the UX-7V longitudinal mode, in addition to using elevons for up and down motion, which also uses differential thrust. This is because the UX-7V longitudinal mode is less stable at the beginning of development. Therefore, it needs to be assisted by other actuators. The use of differential thrust is a tiny amount, a maximum of 10 percent of the total thrust of the brushless motor. Nevertheless, the effect is quite significant because it can be called active control [89]. This differential thrust factor was not modeled in analytical modeling; therefore, the three parameters (related to the angular velocity and angular position) in this longitudinal mode are not identical.

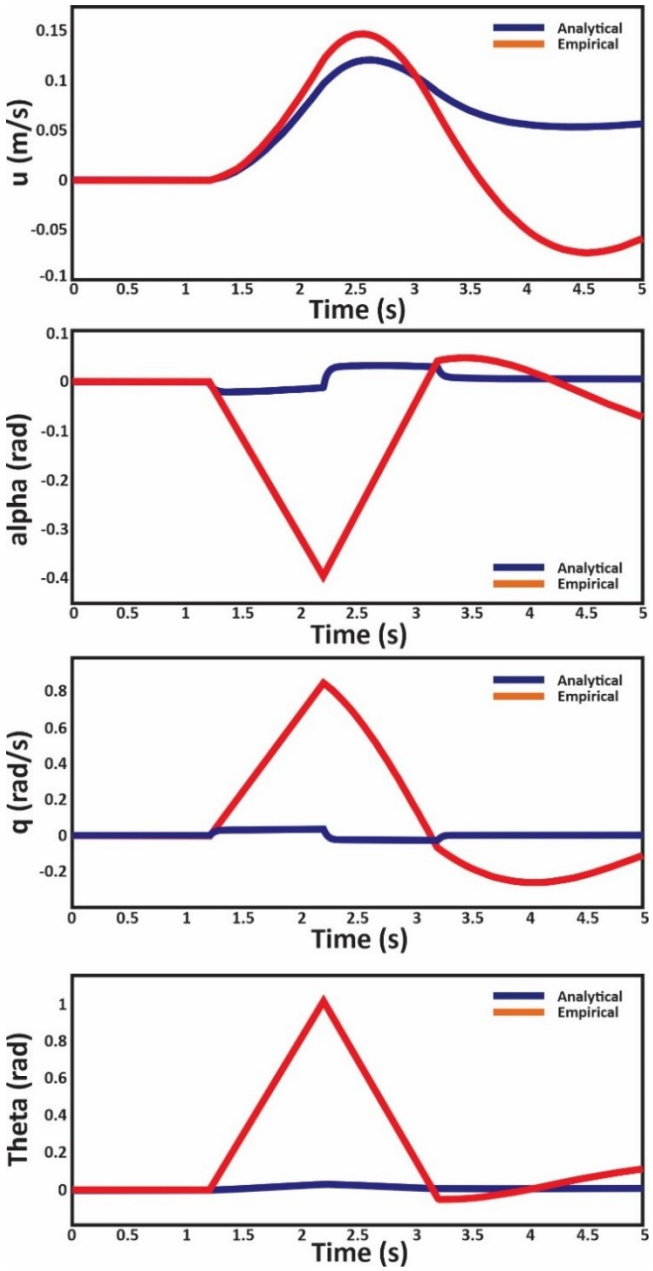

Fig. 22. Longitudinal mode validation results: analytical models (blue) and empirical model (red)

Validation process of the lateral mode is similar with the longitudinal mode, but there is a little different in the doublet input that connected the empirical and analytical models, which is aileron control surface. Both models are also having a state-space model structure. The four output parameters of the model, namely β sideslip angle, p roll angular velocity, r yaw angular velocity, and roll (Φ) angle, are then also displayed in graphical form and stored for further analysis. An analytical model validation in lateral mode MATLAB/Simulink block diagram is shown in Fig. 23.

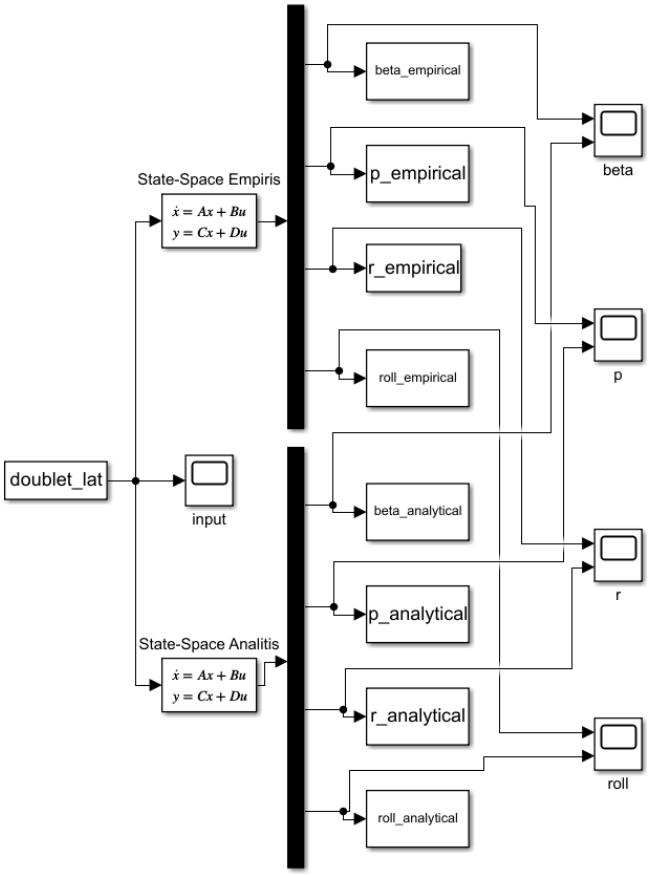

Fig. 23. Lateral mode validation Simulink block diagram

Fig. 24 shows the validation results for the lateral mode, where all four parameters (beta (β), p, r, and roll (Φ)) are identical, showing only a slight delay or lower amplitude in the empirical model. It is normal and can be caused by natural factors, such as wind. Owing to the wind, the aircraft turn maneuver command will be affected, such that the aircraft's response will be a bit late or faster, depending on the wind direction and velocity. Flight data acquisition was designed to be performed in the morning when the weather was sunny and the wind was near zero. Unfortunately, the actual weather conditions of the flight level can differ from those of the ground level.

Based on the results obtained from this research, in general it is better than those produced by previous research [46]. In the empirical model. the improvement is very significant, then in the analytical model, especially in the lateral mode, it is also quite significant. In the longitudinal mode analytical model there are several things that might improve the accuracy and quality of the model, including by entering the propulsion and propeller models used.

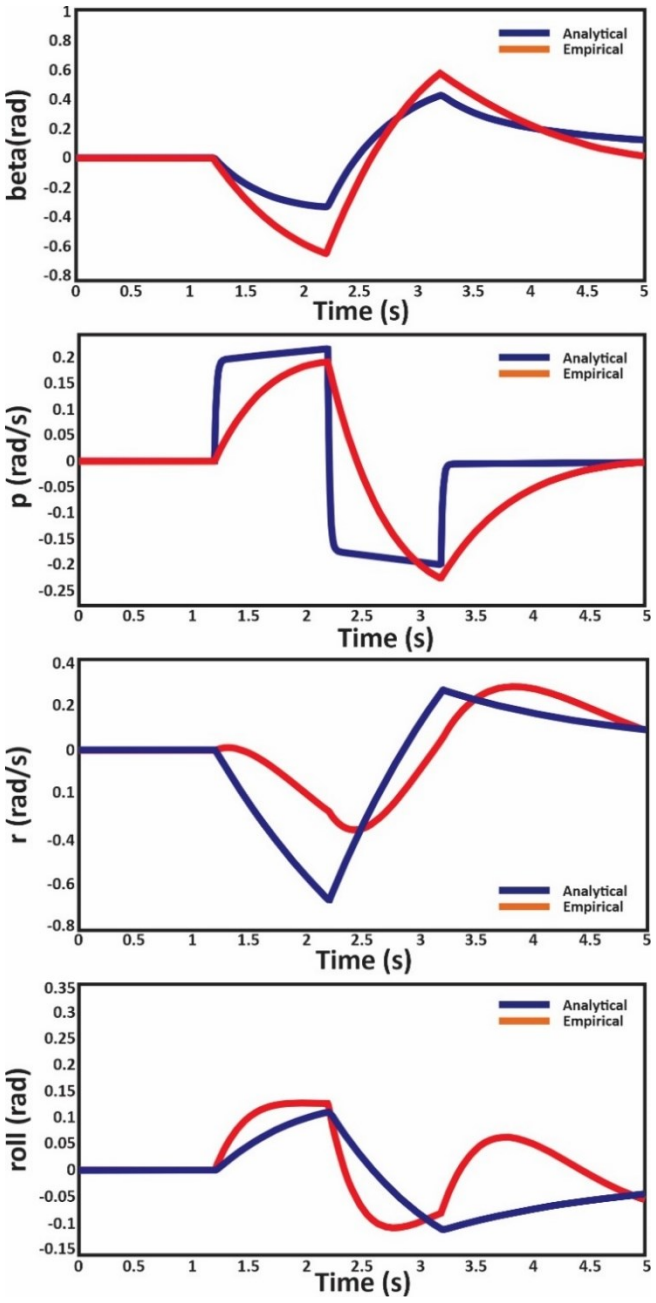

Fig. 24. Lateral mode validation results: analytical models (blue) and empirical model (red)

V. CONCLUSIONS

In this paper, the analytical model of the UX-7V VTOL UAV in fixed-wing mode have been developed using aerodynamic coefficients obtained from OpenVSP. For validating the analytical model, empirical models have been developed from flight data. The validation results showed that the developed analytical model could validly represent the attitude of the UX-7V UAV. Thus, this model can be used directly as the basis for developing the UX-7V control system. Adjustment to the empirical model significantly increased the accuracy of the model. In future research, the

accuracy of the analytical model will be improved by considering the effect of using differential thrust control. Further studies also need to be carried out, although the modeling is more complex, which combines fixed wing [90][91] and copter control [92][93][94], as well as aircraft transition phase [95]. The ultimate and main goal in UAV modeling and simulation is to create a safe and reliable system with a fast time [96]. The obtained model will use for simulation in the specific and even in dangerous condition [97][98][99]. For example, in longitudinal mode will simulate altitude and speed control simulation, whereas in lateral mode will simulate heading control simulation. The simulation will be carried out in normal to dangerous environmental conditions such as strong winds [100].

ACKNOWLEDGMENT

Thanks to the Department of Computer Science and Electronics, Faculty of Mathematics and Natural Science, Universitas Gadjah Mada (UGM), for research funding under contract number 253/J01.1.28/PL.06.02/2022 and technical support.

REFERENCES

[1] D. M. Harfina, Z. Zaini, and W. J. Wulung, "Disinfectant spraying system with quadcopter type unmanned aerial vehicle technology as an effort to break the chain of the covid-19 virus," *J. Robot. Control*, vol. 2, no. 6, pp. 502–507, 2021, doi: 10.18196/jrc.26129.

[2] W. Rahmaniar and A. E. Rakhmania, "Online digital image stabilization for an unmanned aerial vehicle (UAV)," *J. Robot. Control*, vol. 2, no. 4, pp. 234–239, 2021, doi: 10.18196/jrc.2484.

[3] A. Alcántara, J. Capitán, R. Cunha, and A. Ollero, "Optimal trajectory planning for cinematography with multiple Unmanned Aerial Vehicles," *Rob. Auton. Syst*., vol. 140, p. 103778, 2021, doi: 10.1016/j.robot.2021.103778.

[4] R. Bailon-Ruiz, A. Bit-Monnot, and S. Lacroix, "Real-time wildfire monitoring with a fleet of UAVs," *Rob. Auton. Syst.*, vol. 152, p. 104071, 2022, doi: 10.1016/j.robot.2022.104071.

[5] D. Jo and Y. Kwon, "Development of Autonomous VTOL UAV for Wide Area Surveillance," *World J. Eng. Technol.*, vol. 7, no. 1, pp. 227-239, 2019, doi: 10.4236/wjet.2019.71015.

[6] T. Y. Erkec and C. Hajiyev, "Relative Navigation in UAV Applications," *Int. J. Aviat. Sci. Technol.*, vol. 1, no. 2, pp. 52-65, 2020, doi: 10.23890/IJAST.vm01is02.0202.

[7] H. N. Qureshi and A. Imran, "On the Tradeoffs between Coverage Radius, Altitude, and Beamwidth for Practical UAV Deployments," *IEEE Trans. Aerosp. Electron. Syst.*, vol. 55, no. 6, pp. 2805–2821, 2019, doi: 10.1109/TAES.2019.2893082.

[8] Z. Xiong, Y. Xu, Z. Wang, X. Pian, and Y. Wang, "Preliminary Design Method and Prototype Testing of a Novel Rotors Retractable Hybrid VTOL UAV," in *IEEE Access*, vol. 9, pp. 161141-161160, 2021, doi: 10.1109/ACCESS.2021.3131565.

[9] Q. Xia, S. Liu, M. Guo, H. Wang, Q. Zhou, and X. Zhang, "Multi-UAV trajectory planning using gradient-based sequence minimal optimization," *Rob. Auton. Syst.*, vol. 137, p. 103728, 2021, doi: 10.1016/j.robot.2021.103728.

[10] S. Garcia-Nieto, J. Velasco-Carrau, F. Paredes-Valles, J. V. Salcedo, and R. Simarro, "Motion Equations and Attitude Control in the Vertical Flight of a VTOL Bi-Rotor UAV," *Electronics*, vol. 8, p. 208, 2019, doi: 10.3390/electronics8020208

[11] L. Bauersfeld, L. Spannagl, G. Ducard, and C. Onder, "MPC Flight Control for a Tilt-Rotor VTOL Aircraft," *IEEE Trans. Aerosp. Electron. Syst.*, vol. 57, no. 4, pp. 2395–2409, 2021, doi: 10.1109/TAES.2021.3061819.

[12] M. F. Bornebusch and T. A. Johansen, "Autonomous Recovery of a Fixed-Wing UAV Using a Line Suspended between Two Multirotor UAVs," *IEEE Trans. Aerosp. Electron. Syst.*, vol. 57, no. 1, pp. 90–104, 2021, doi: 10.1109/TAES.2020.3009509.

[13] Y. Byun, J. Song, W. Song, and B. Kang, "Conceptual Study of a Smart Docking System for VTOL-UAV," *J. Aerosp. Eng.*, vol. 29, no. 2, 2016, doi:10.1061/(ASCE)AS.1943-5525.0000508.

[14] Q. Chen, M. Tao, X. He, and L. Tao, "Fuzzy Adaptive Nonsingular Fixed-Time Attitude Tracking Control of Quadrotor UAVs," *IEEE Trans. Aerosp. Electron. Syst.*, vol. 57, no. 5, pp. 2864–2877, 2021, doi: 10.1109/TAES.2021.3067610.

[15] M. R. Cohen and J. R. Forbes, "Navigation and Control of Unconventional VTOL UAVs in Forward-Flight with Explicit Wind Velocity Estimation," *IEEE Robot. Autom. Lett.*, vol. 5, no. 2, 2020, doi: 10.1109/LRA.2020.2966406.

[16] Q. Chen, Y. Ye, Z. Hu, J. Na, and S. Wang, "Finite-Time Approximation-Free Attitude Control of Quadrotors: Theory and Experiments," *IEEE Trans. Aerosp. Electron. Syst.*, vol. 57, no. 3, pp. 1780–1792, 2021, doi: 10.1109/TAES.2021.3050647.

[17] R. Gill and R. D'andrea, "An annular wing VTOL UAV: Flight dynamics and control," *Drones*, vol. 4, no. 2, 2020, doi: 10.3390/drones4020014.

[18] A. González-Sieira, D. Cores, M. Mucientes, and A. Bugarín, "Autonomous navigation for UAVs managing motion and sensing uncertainty," *Rob. Auton. Syst.*, vol. 126, p. 103455, 2020, doi: 10.1016/j.robot.2020.103455.

[19] J. Han, L. Di, C. Coopmans, and Y. Chen, "Pitch loop control of a VTOL UAV using fractional order controller," *J. Intell. Robot. Syst. Theory Appl.*, vol. 73, no. 187-195, 2014, doi: 10.1007/s10846-013-9912-9.

[20] H. Abrougui, S. Nejim, and H. Dallagi, "Roll Control of a Tail-Sitter VTOL UAV," *Int. J. Control. Energy Electr. Eng.*, vol. 7, 2019.

[21] R. B. Anderson, J. A. Marshall, and A. L'Afflitto, "Constrained Robust Model Reference Adaptive Control of a Tilt-Rotor Quadcopter Pulling an Unmodeled Cart," *IEEE Trans. Aerosp. Electron. Syst.*, vol. 57, no. 1, pp. 39–54, 2021, doi: 10.1109/TAES.2020.3008575.

[22] L. Pugi *et al.*, "Preliminary Design and Simulation of an Hybrid-Parallel, Fixed-Wing UAV with Eight-Rotors VTOL System," in *2022 IEEE International Conference on Environment and Electrical Engineering and 2022 IEEE Industrial and Commercial Power Systems Europe (EEEIC / I&CPS Europe)*, pp. 1-6, 2022, doi: 10.1109/EEEIC/ICPSEurope54979.2022.9854554.

[23] K. M. Min, F. Y. Chia, and B. H. Kim, "Design and CFD analysis of a low-altitude VTOL UAV," *Int. J. Mech. Prod. Eng. Res. Dev.*, vol. 9, no. 2, 2018, doi: 10.24247/ijmperdapr201954.

[24] K. M. Min, F. Y. Chia, and B. H. Kim, "Development of VTOL UAV with module for direction finding," *Int. J. Mech. Prod. Eng. Res. Dev.*, vol. 9, no. 3, 2019.

[25] V. Nekoukar and N. Mahdian Dehkordi, "Robust path tracking of a quadrotor using adaptive fuzzy terminal sliding mode control," *Control Eng. Pract.*, vol. 110, p. 104763, 2021, doi: 10.1016/j.conengprac.2021.104763.

[26] A. Prach and E. Kayacan, "An MPC-based position controller for a tilt-rotor tricopter VTOL UAV," *Optim. Control Appl. Methods*, vol. 39, no. 1, pp. 343–356, 2018, doi: 10.1002/oca.2350.

[27] C. Sastre, J. Wubben, C. T. Calafate, J. C. Cano, and P. Manzoni, "Safe and Efficient Take-Off of VTOL UAV Swarms," *Electronics*, vol. 11, p. 1128, 2022, doi: 10.3390/electronics11071128.

[28] Z. Cheng, H. Pei, and S. Li, "Neural-Networks Control for Hover to High-Speed-Level-Flight Transition of Ducted Fan UAV With Provable Stability," in *IEEE Access*, vol. 8, pp. 100135-100151, 2020, doi: 10.1109/ACCESS.2020.2997877.

[29] S. Q. Sohail, F. Akram, N. Hussain, and A. Shahzad, "Design and Transition of a Quad Rotor Tail-sitter VTOL UAV with Experimental Verification," *International Bhurban Conference on Applied Sciences and Technologies (IBCAST)*, pp. 244-251, 2021, doi: 10.1109/IBCAST51254.2021.9393187.

[30] L. Wu, C. Li, Q. Ding, C. Wang, L. Zhu, and X. Tan, "VTOL Control of Tailsitter UAV Under Crosswind Disturbances," in *Chinese Control and Decision Conference (CCDC)*, pp. 2776-2781, 2020, doi: 10.1109/CCDC49329.2020.9164116.

[31] B. Li, J. Sun, W. Zhou, C. -Y. Wen, K. H. Low, and C. -K. Chen, "Transition Optimization for a VTOL Tail-Sitter UAV," in *IEEE/ASME Transactions on Mechatronics*, vol. 25, no. 5, pp. 2534-2545, 2020, doi: 10.1109/TMECH.2020.2983255.

[32] K. McIntosh, J. -P. Reddinger, and S. Mishra, "A Switching-Free Control Architecture for Transition Maneuvers of a Quadrotor Biplane Tailsitter," *American Control Conference (ACC)*, pp. 4011-4016, 2022, doi: 10.23919/ACC53348.2022.9867242

[33] Y. Mansor, Z. Sahwee, and M. H. M. Asri, "Development of Multiple Configuration Flying Wing UAV," in *International Conference on Computer and Drone Applications (IConDA)*, pp. 9-12, 2019, doi: 10.1109/IConDA47345.2019.9034911.

[34] R. Aarenstrup, *Managing Model Based Design*, Natick: The MathWorks, Inc, 2015.

[35] Y. Ke, K. Wang, and B. M. Chen, "Design and Implementation of a Hybrid UAV With Model-Based Flight Capabilities," *IEEE/ASME Transactions on Mechatronics*, vol. 23, no. 3, pp. 1114-1125, 2018, doi: 10.1109/TMECH.2018.2820222.

[36] D. Rohr, M. Studiger, T. Stastny, N. R. J. Lawrance, and R. Siegwart, "Nonlinear Model Predictive Velocity Control of a VTOL Tiltwing UAV," in *IEEE Robotics and Automation Letters*, vol. 6, no. 3, pp. 5776-5783, 2021, doi: 10.1109/LRA.2021.3084888.

[37] S. J. Carlson and C. Papachristos, "The MiniHawk-VTOL: Design, Modeling, and Experiments of a Rapidly-prototyped Tiltrotor UAV," *International Conference on Unmanned Aircraft Systems (ICUAS)*, pp. 777-786, 2021, doi: 10.1109/ICUAS51884.2021.9476731.

[38] N. B. F. Silva, J. V. C. Fontes, and K. R. L. J. C. Branco, "Control validation with software-in-the-loop for a fixed-wing vertical takeoff and landing unmanned aerial vehicle with multiple flight stages," *IEEE Symposium on Computers and Communications (ISCC)*, pp. 1222-1227, 2019, doi: 10.1109/ISCC47284.2019.8969571.

[39] C. Gellida-Coutiño, V. D. -D. La Cruz, A. Sanchez-Orta, O. Garcia-Salazar, and P. Castillo, "The tailsitter autogiro UAV: modeling, design, and CFD simulation," *International Conference on Unmanned Aircraft Systems (ICUAS)*, pp. 516-525, 2022, doi: 10.1109/ICUAS54217.2022.9836091.

[40] Z. Zaludin, C. Chia, and E. Abdullah, "Non-Linear Analytical Mathematical Modelling of a Hybrid Fixed-Wing Unmanned Aerial Vehicle in Pusher Configuration," in *IEEE International Conference on Automatic Control & Intelligent Systems (I2CACIS)*, pp. 1-6, 2021, doi: 10.1109/I2CACIS52118.2021.9495891.

[41] Napolitano, *Aircraft Dynamics From Modeling to Simulation*, New Jersey: John Wiley & Sons, 2012.

[42] R. Chiappinelli and M. Nahon, "Modeling and Control of a Tailsitter UAV," in *International Conference on Unmanned Aircraft Systems (ICUAS)*, pp. 400-409, 2018, doi: 10.1109/ICUAS.2018.8453301.

[43] T. K. Priyambodo, A. Dharmawan, O. A. Dhewa, and N. A. S. Putro, "Design of Flight Control System for Flying Wing UAV Based on Pitch and Roll Rotation," *Int. J. of Eng. Res. and Management (IJERM)*, vol. 3, pp 51-54, 2016.

[44] X. Lyu, H. Gu, Y. Wang, Z. Li, S. Shen, and F. Zhang, "Design and implementation of a quadrotor tail-sitter VTOL UAV." in *IEEE International Conference on Robotics and Automation (ICRA)*, pp. 3924-3930, 2017, doi: 10.1109/ICRA.2017.7989452.

[45] A. Oosedo, S. Abiko, A. Konno, T. Koizumi, T. Furui, and M. Uchiyama, "Development of a quad rotor tail-sitter VTOL UAV without control surfaces and experimental verification," in *IEEE International Conference on Robotics and Automation*, pp. 317-322, 2013, doi: 10.1109/ICRA.2013.6630594.

[46] T. K. Priyambodo and A. Majid, "Modeling and Simulation of the UX-6 Fixed-Wing Unmanned Aerial Vehicle," *J Control Autom Electr Syst*., vol. 32, pp. 1344–1355, 2021, doi: 0.1007/s40313-021-00754-5.

[47] R. A. McDonald, "Advanced modeling in OpenVSP," in *Proceedings of 16th AIAA Aviation Technology, Integration, and Operations Conference Exposition*, pp. 1-6, 2016, doi: 10.2514/6.2016-3282.

[48] K. S. Lelkov, D. V. Ulyanov, D. A. Surkov, and A. N. Ushakov, "Development of the mathematical model for the tilt-rotor aircraft," in *19th International Conference "Aviation and Cosmonautics*, pp. 1-9, 2020, doi: 10.1088/1742-6596/1925/1/012041.

[49] I. Staack, R.C. Munjulury, T. Melin, A. Abdalla, and P. Krus, "Conceptual Design Model Management Demonstrated on a 4th Generation Fighter," in *Proceedings of 29th International Council of the Aeronautical Science*, pp. 1-9, 2014.

[50] S. I. Azid, K. Kumar, M. Cirrincione, and A. Fagiolini, "Wind gust estimation for precise quasi-hovering control of quadrotor aircraft," *Control Eng. Pract.*, vol. 116, p. 104930, 2021, doi: 10.1016/j.conengprac.2021.104930.

[51] G. Frontera, I. Campana, A. M. Bernardos, and J. A. Besada, "Formal Intent-Based Trajectory Description Languages for Quadrotor Aircraft," *IEEE Trans. Aerosp. Electron. Syst.,* vol. 55, no. 6, pp. 3330–3346, 2019, doi: 10.1109/TAES.2019.2907396.

[52] N. T. Hegde, V. I. George, C. G. Nayak, and K. Kumar, "Design, dynamic modelling and control of tilt-rotor UAVs: a review," *International Journal of Intelligent Unmanned Systems*, vol. 8, no. 3, pp. 143–161, 2020, doi: /10.1108/IJIUS-01-2019-0001.

[53] Y. Hu, K. Shen, K. A. Neusypin, A. V. Proletarsky, and M. S. Selezneva, "Hierarchic Controllability Analysis in High-Dynamic Guidance for Autonomous Vehicle Landing," *IEEE Trans. Aerosp. Electron. Syst.*, vol. 58, no. 3, pp. 1545–1557, 2022, doi: 10.1109/TAES.2021.3122918.

[54] R. Ji, J. Ma, and S. Sam Ge, "Modeling and Control of a Tilting Quadcopter," *IEEE Trans. Aerosp. Electron. Syst.*, vol. 56, no. 4, pp. 2823–2834, 2020, doi: 10.1109/TAES.2019.2955525.

[55] A. Rasheed, "Grey box identification approach for longitudinal and lateral dynamics of UAV," *International Conference on Open Source Systems & Technologies (ICOSST)*, pp. 10-14, 2017, doi:10.1109/ICOSST.2017.8278998.

[56] L. Wu, H. Li, Y. Li, and C. Li, "Position Tracking Control of Tailsitter VTOL UAV With Bounded Thrust-Vectoring Propulsion System," in *IEEE Access*, vol. 7, pp. 137054-137064, 2019, doi: 10.1109/ACCESS.2019.2942526.

[57] M. B. Tischler, *Aircraft and Rotorcraft System Identification, Engineering Methods with Flight Test Example*, Virginia: American Institute of Aeronautics and Astronautics, 2006.

[58] O. Mechali, L. Xu, Y. Huang, M. Shi, and X. Xie, "Observer-based fixed-time continuous nonsingular terminal sliding mode control of quadrotor aircraft under uncertainties and disturbances for robust trajectory tracking: Theory and experiment," *Control Eng. Pract.*, vol. 111, p. 104806, 2021.

[59] A. L. Silva and D. A. Santos, "Fast Nonsingular Terminal Sliding Mode Flight Control for Multirotor Aerial Vehicles," *IEEE Trans. Aerosp. Electron. Syst.*, vol. 56, no. 6, pp. 4288–4299, 2020, doi: 10.1109/TAES.2020.2988836.

[60] T. Souanef, "L1 Adaptive Path-Following of Small Fixed-Wing Unmanned Aerial Vehicles in Wind," *IEEE Trans. Aerosp. Electron. Syst.*, vol. 58, no. 4, pp. 3708–3716, 2022, doi: 10.1109/TAES.2022.3153758.

[61] M. Tao, Q. Chen, X. He, and S. Xie, "Fixed-Time Filtered Adaptive Parameter Estimation and Attitude Control for Quadrotor UAVs," *IEEE Trans. Aerosp. Electron. Syst.*, vol. 58, no. 5, pp. 4135–4146, 2022, doi: 10.1109/TAES.2022.3159770.

[62] J. Yang, Z. Cai, J. Zhao, Z. Wang, Y. Ding, and Y. Wang, "INDI-based aggressive quadrotor flight control with position and attitude constraints," *Rob. Auton. Syst.*, vol. 159, p. 104292, 2023, doi: 10.1016/j.robot.2022.104292.

[63] B. L. Stevens and F. L. Lewis, *Aircraft Control and Simulation*, 2nd ed., New Jersey: John Wiley & Sons, Inc, 2003.

[64] R. C. Nelson, *Flight Stability and Automatic Control*, 2nd ed., Colombus: McGraw-Hill Int, 1998.

[65] M. S. Roeser and N. Fezans, "Method for designing multi-input system identification signals using a compact time-frequency representation," *CEAS Aeronautical Journal*, vol. 12, pp. 291–306, 2021, doi: 10.1007/s13272-021-00499-6.

[66] M. S. Smith and T. R. Moes, "Real-time Stability and Control Derivative Extraction from F15 Flight Data," in *Proceedings of AIAA Atmospheric Flight Mechanics Conference*, pp. 1-31, 2003, doi: 10.2514/6.2003-5701.

[67] C. Ben Jabeur and H. Seddik, "Optimized Neural Networks-PID Controller with Wind Rejection Strategy for a Quad-Rotor," *J. Robot. Control*, vol. 3, no. 1, pp. 62–72, 2022, doi: 10.18196/jrc.v3i1.11660.

[68] K. Kim, S. Kim, J. Suk, J. Ahn, N. Kim, and B-S. Kim, Flight test of flying-wing type unmanned aerial vehicle with partial wing-loss. *Journal of Aerospace Engineering*, vol. 233, no. 5, pp. 1611-1628, 2018, doi:10.1177/0954410018758497.

[69] M. Liu, G. K. Egan, and F. Santoso, "Modeling, Autopilot Design, and Field Tuning of a UAV With Minimum Control Surfaces," in *IEEE*

Transactions on Control Systems Technology, vol. 23, no. 6, pp. 2353-2360, 2015, doi: 10.1109/TCST.2015.2398316.

[70] B. Li, W. Gong, Y. Yang, B. Xiao, and D. Ran, "Appointed Fixed Time Observer-Based Sliding Mode Control for a Quadrotor UAV under External Disturbances," *IEEE Trans. Aerosp. Electron. Syst.*, vol. 58, no. 1, pp. 290–303, 2022, doi: 10.1109/TAES.2021.3101562.

[71] Y. Zou and K. Xia, "Robust fault-tolerant control for underactuated takeoff and landing UAVs," *IEEE Trans. Aerosp. Electron. Syst.*, vol. 56, no. 5, pp. 3545–3555, 2020, doi: 10.1109/TAES.2020.2975446.

[72] W. Zhou, S. Chen, C. -W. Chang, C. -Y. Wen, C. -K. Chen, and B. Li, "System Identification and Control for a Tail-Sitter Unmanned Aerial Vehicle in the Cruise Flight," in *IEEE Access*, vol. 8, pp. 218348-218359, 2020, doi: 10.1109/ACCESS.2020.3042316.

[73] W. Xu and F. Zhang, "Learning Pugachev's Cobra Maneuver for Tail-Sitter UAVs Using Acceleration Model," in *IEEE Robotics and Automation Letters*, vol. 5, no. 2, pp. 3452-3459, 2020, doi: 10.1109/LRA.2020.2976323.

[74] A. Mansour, A. M. Kamel, and E. Safwat, "System Identification and Modeling of an Actuation System for Small Aerial Vehicle," in *13th International Conference on Electrical Engineering (ICEENG)*, pp. 5-8, 2022, doi: 10.1109/ICEENG49683.2022.9782039.

[75] S. Sakulthong, S. Tantrairatn, and W. Saengphet, "Frequency Response System Identification and Flight Controller Tuning for Quadcopter UAV," in *Third International Conference on Engineering Science and Innovative Technology (ESIT)*, pp. 1-6, 2018, doi: 10.1109/ESIT.2018.8665114.

[76] D. Reinhardt, K. Gryte, and T. Arne Johansen, "Modeling of the Skywalker X8 Fixed-Wing UAV: Flight Tests and System Identification," in *International Conference on Unmanned Aircraft Systems (ICUAS)*, pp. 506-515, 2022, doi: 10.1109/ICUAS54217.2022.9836104.

[77] D. Rose. (2015). *Rotation Quaternion, and How to Use Them* [online]: https://danceswithcode.net/engineeringnotes/quaternions/quaternions.html

[78] J. Zhou, X. Lyu, X. Cai, Z. Li, S. Shen, and F. Zhang, "Frequency domain model identification and loop-shaping controller design for quadrotor tail-sitter VTOL UAVs," in *International Conference on Unmanned Aircraft Systems (ICUAS)*, pp. 1142-1149, 2018, doi: 10.1109/ICUAS.2018.8453475

[79] F. R. Triputra, B. R. Trilaksono, R. A. Sasongko, and M. Dahsyat, "Longitudinal dynamic system modeling of a fixed-wing UAV towards autonomous flight control system development: A case study of BPPT Wulung UAV platform 2012," in *International Conference on System Engineering and Technology (ICSET)*, pp. 1-6, 2012, doi: 10.1109/ICSEngT.2012.6339294.

[80] A. Majid, R. Sumiharto, and S. B. Wibowo, "Identifikasi Model Dari Pesawat Udara Tanpa Awak Sayap Tetap Jenis Bixler," *Indonesian Journal of Electronics Instrumentation System (IJEIS)*, vol. 5, pp. 43–54, 2015, doi: 10.22146/ijeis.7152.

[81] K. T. Borup, T. I. Fossen, and T. A. Johansen, "A machine learning approach for estimating air data parameters of small fixed-wing UAVs using distributed pressure sensors," *IEEE Trans. Aerosp. Electron. Syst.*, vol. 56, no. 3, pp. 2157–2173, 2020, doi: 10.1109/TAES.2019.2945383.

[82] J. Tupy and I. Zelinka, "Evolutionary Algorithms in Aircraft Trim Optimization," *2008 19th International Workshop on Database and Expert Systems Applications*, pp. 524-530, 2008, doi: 10.1109/DEXA.2008.98.

[83] C. Jouannet, P. Berry, T. Melin, K. Amadori, D. Lundström, and I. Staack, "Subscale flight testing used in conceptual design," *Aircraft Engineering and Aerospace Technology*, vol. 84, pp. 192-199, 2021, doi: 10.1108/00022661211222058.

[84] L. Wu, H. Li, Y. Li, and C. Li, "Position Tracking Control of Tailsitter VTOL UAV With Bounded Thrust-Vectoring Propulsion System," in *IEEE Access*, vol. 7, pp. 137054-137064, 2019, doi: 10.1109/ACCESS.2019.2942526.

[85] Y. Bouzid, H. Siguerdidjane, and Y. Bestaoui, "Generic dynamic modeling for multirotor VTOL UAVs and robust Sliding Mode based Model-Free Control for 3D navigation," in *International Conference on Unmanned Aircraft Systems (ICUAS)*, pp. 970-979, 2018, doi: 10.1109/ICUAS.2018.8453293.

[86] M. R. Cohen and J. R. Forbes, "Navigation and Control of Unconventional VTOL UAVs in Forward-Flight with Explicit Wind Velocity Estimation," in *IEEE Robotics and Automation Letters*, vol. 5, no. 2, pp. 1151-1158, 2020, doi: 10.1109/LRA.2020.2966406.

[87] L. M. Sánchez-Rivera, R. Lozano, and A. Arias-Montano, "Pitching moment analysis and adjustment for tilt-wing UAV in VTOL mode," *International Conference on Unmanned Aircraft Systems (ICUAS)*, pp. 1445-1450, 2019, doi: 10.1109/ICUAS.2019.8797952.

[88] G. D. Santos, A. Kossoski, J. Balthazar, and A. M. Tusset, "SDRE and LQR Controls Comparison Applied in High-Performance Aircraft in a Longitudinal Flight," *International Journal of Robotics and Control Systems*, vol. 1, no. 2, pp. 131-144, 2021, doi: 10.31763/ijrcs.v1i2.329.

[89] A. N. De Lucena, B. M. F. Da Silva, and L. M. G. Gonçalves, "Double Hybrid Tailsitter Unmanned Aerial Vehicle with Vertical Takeoff and Landing," in *IEEE Access*, vol. 10, pp. 32938-32953, 2022, doi: 10.1109/ACCESS.2022.3161490.

[90] W. Premerlani, J. Ingersoll, S. Edwards, M. Darnell, and S. Ali, "Multi-Axis Control for Small UAS VTOL Autopilot," in *AIAA/IEEE 39th Digital Avionics Systems Conference (DASC)*, pp. 1-10, 2020, doi: 10.1109/DASC50938.2020.9256535.

[91] J. Sun, B. Li, C. -Y. Wen, and C. -K. Chen, "Model-Aided Wind Estimation Method for a Tail-Sitter Aircraft," in *IEEE Transactions on Aerospace and Electronic Systems*, vol. 56, no. 2, pp. 1262-1278, 2020, doi: 10.1109/TAES.2019.2929379.

[92] M. Maaruf, M. S. Mahmoud, and A. Ma'arif, "A Survey of Control Methods for Quadrotor UAV," *International Journal of Robotics and Control Systems*, vol. 2, no. 4, pp. 652-665, 2022, https://doi.org/10.31763/ijrcs.v2i4.743.

[93] I. Ahmad, M. Liaquat, F. M. Malik, H. Ullah, and U. Ali, "Variants of the Sliding Mode Control in Presence of External Disturbance for Quadrotor," in *IEEE Access*, vol. 8, pp. 227810-227824, 2020, doi: 10.1109/ACCESS.2020.3041678.

[94] Y. Yang, J. Zhu, X. Zhang, and X. Wang, "Active Disturbance Rejection Control of a Flying-Wing Tailsitter in Hover Flight," in *IEEE/RSJ International Conference on Intelligent Robots and Systems (IROS)*, pp. 6390-6396, 2018, doi: 10.1109/IROS.2018.8594470.

[95] S. M. Nogar and C. M. Kroninger, "Development of a Hybrid Micro Air Vehicle Capable of Controlled Transition," in *IEEE Robotics and Automation Letters*, vol. 3, no. 3, pp. 2269-2276, 2018, doi: 10.1109/LRA.2018.2800797.

[96] I. Iriarte, I. Iglesias, J. Lasa, H. Calvo-Soraluze, and B. Sierra, "Enhancing VTOL Multirotor Performance with a Passive Rotor Tilting Mechanism," in *IEEE Access*, vol. 9, pp. 64368-64380, 2021, doi: 10.1109/ACCESS.2021.3075113.

[97] S. Fuhrer, S. Verling, T. Stastny, and R. Siegwart, "Fault-tolerant Flight Control of a VTOL Tailsitter UAV," *International Conference on Robotics and Automation (ICRA)*, pp. 4134-4140, 2019, doi: 10.1109/ICRA.2019.8793467.

[98] G. Ortiz-Torres *et al*., "Fault Estimation and Fault Tolerant Control Strategies Applied to VTOL Aerial Vehicles with Soft and Aggressive Actuator Faults," in *IEEE Access*, vol. 8, pp. 10649-10661, 2020, doi: 10.1109/ACCESS.2019.2963693.

[99] B. Wang, D. Zhu, L. Han, H. Gao, Z. Gao, and Y. Zhang, "Adaptive Fault-Tolerant Control of a Hybrid Canard Rotor/Wing UAV Under Transition Flight Subject to Actuator Faults and Model Uncertainties," in *IEEE Transactions on Aerospace and Electronic Systems*, pp. 1-16, 2023, doi: 10.1109/TAES.2023.3243580.

[100] Y. Hou, W. Huang, H. Zhou, F. Gu, Y. Chang, and Y. He, "Analysis on Wind Resistance Index of Multi-rotor UAV," in *Chinese Control and Decision Conference (CCDC)*, pp. 3693-3696, 2019, doi: 10.1109/CCDC.2019.8832752.